nature portfolio

Peer Review File

PTPRK regulates glycolysis and de novo lipogenesis to promote hepatocyte metabolic reprogramming in obesity

Corresponding Author: Dr Esteban Gurzov

This file contains all reviewer reports in order by version, followed by all author rebuttals in order by version.

Version 0:

Reviewer comments:

Reviewer #1

(Remarks to the Author)
This is an interesting, very well written paper focusing on the characterization of the role of PTPRK in hepatocytes. There is a lot of data and the key findings are that PTPRK is upregulated in steatosis and NASH, where it regulates hepatocyte metabolism to promote lipogenesis. This part is elegantly demonstrated via genomics, metabolomics, and in vivo experiments using KO mice and ad-PTPRK expression systems. The authors then provide evidence -unfortunately a bit weak- that such effect of PTPRK is due to dephosphorylation of FBP1, a key glycolysis enzyme. Finally, they report evidence that deletion of PTPRK mildly affects dinitrosamine tumorigenesis in mice. Strengths of the paper are the fact that human specimens and data analysis guided mouse and cell biology experimentation and the meticulous experimentation. However the paper needs a bit more work to support mechanistic conclusions about how PTPRK regulates lipogenesis in hepatocytes.

Major comments

The molecular biology part of the paper (i.e. the identification of a new substrate of PTPRK) is an essential part of the novelty and depth of this paper but is weak at the moment and needs further elaboration and experimentation. Are the site identified exposed in structures of FBP1 (from my preliminary assessment Y265 might have limited exposure)? The models provided need to be shown at much higher resolution and what is the predicted effect of phosphorylation on the structure of FBP1? Much more evidence of FBP1 phosphorylation endogenously as well as dephosphorylation by D1+D2 PTPRK needs to be provided. Ideally also expression of phosphorylation-deficient mutants of FBP1 would be provided in order to support that FBP1 is key in mediating the mechanism of action of PTPRK.

Another significant weakness is the lack of any discussion of limitations/inconsistent areas of the study. For example what's the meaning of differences that are only evident when comparing high fat vs low fat hepatocytes within genotypes, or why there is a dissociation between enzyme and metabolite expression in Fig. 6D, or why the tumorigenesis phenotype in the last figure is so mild (is there any compensation mechanism?)

The figures legends needs to be more detailed in explaining 1) the content of the panels, for example Fig. 1F is that protein or mRNA data? 2) What statistics have been utilized in the figure, 3) for non in vivo experiments whether the replicates were done using lines from different mice or same line different experiments or were they technical replicates, 4) where mixed M and F mice have been utilized (Fig. 4E?) and where not.

Minor comments

1. The figures are too dense and some panels can be eliminated, for example the scheme in Fig. 1C can be replaced by a scheme of PTPRK.

2. Fig 1 G. The text mentions that the figure only reports PTPRK.

3. Fig. 1J. IHC is not quantitative and the observation of nuclear-only overexpression is not easily rationalized, also is there any data about the validation of the antibody utilized? This figure ideally needs to be replaced by IF on human or mouse specimens and looking at plasma-membrane vs nuclear pattern.

4. Fig, 2I. This is a modest increase, how does it compare to the mass spec data in human tissues.

5. Fig. 2J. The blot seems to show a much higher level of overexpression than even the highest point of the histogram.

6. Fig. 4B. There seems to be two groups of animals here for what concerns SREBP1 expression can the authors comment on it.

7. Fig. 4 G and H, is any metabolic phenotyping available for these mice?

8. Fig. 5F this figure needs a heading.

9. Fig. 7E. The discrepancy between tumor size and area needs some explanation.

Reviewer #2

(Remarks to the Author)
In this work, Gilglioni et al demonstrated that the tyrosine phosphatase receptor PTPRK is mediating liver lipogenesis, steatosis and potentially HCC mediated by MAFLD.

At first, the authors demonstrated an increase in the expression of several PTPRs, but decided to focus on PTPRK as it is the most abundant PTPR in the liver. It is uniquely induced during hepatic steatosis and steatohepatitis, but then downregulated in HCC. The authors directly linked the expression levels of PPARG with that of PTPRK, and with that, correlated PTPRK with metabolic dysregulations observed in fatty live diseases. Using phosphor-proteomics, they also demonstrated that PTPRK is dephosphorylating the gluconeogenic gene FBP1, and with that fructose-1,6-P2 (the substrate of FBP1) is lower in PTPRK knockout cells, indicative of a negative correlation between PTPRK and FBP1 (inactivation of FBP1 by PTPRK). In line with that, PTPRK overexpression stimulated glycolysis.

While the work provides supporting evidence for their conclusions, it is still somewhat correlative in nature, and lack clarity of the mechanism by which PTPRK is involved with MAFLD.

Specific points to address:
1. A technical point: In the PTP proteomics (Figure 1E & F) the results are presented semi-quantitatively where each PTP is compared to other family members. Using “spectral counts” as the authors did, one cannot compare the abundance of different peptides, as they may be ionized differently and provide different counts. Hence, one can only discuss the relative abundance of each protein under different conditions (comparing the signal of identical peptides). This needs clarifications and a different way to present the data – though the conclusions to continue the focus on PTPRK will not change, as they are eventually based on RNA expression levels.

2. The authors did not explain why DMOG was used, and what does it mean to the study. Is PTPRK regulated by dyoxygenases or HIF? The effect of DMOG on PTPRK and PPARG was dramatic nevertheless (more than the Notch inhibitor) and requires explanations.

3. In Figure 3 the authors nicely compared the PTPRK knockout to wt mice under obesity conditions. However, the effects, as significant as they may be, are not compared to non-obese mice (chow diet), hence the reader lack the appreciation of the meaning of these effects. This should be presented.

4. While the work initially demonstrates the correlation between PTPRK and PPARG, it was left unclear how much of the observed PTPRK effect on steatosis is actually mediated via PPARG. This is especially important to appreciate the role of FBP1 in the pathophysiology pf PTPRK expression in fatty liver. Inhibition or ablation of PPARG in ad-PTPRK expressed hepatocytes (preferably in-vivo) would provide a better understanding.

5. In Supplementary Figure 5 the authors analyzed AP-1 levels specifically, but later they used RNAseq (Supplementary Figure 6). Nevertheless, it is unclear whether the RNAseq data actually supported their conclusions that PTPRK mediates a transcriptional cascade orchestrated by PPARG and AP1. This remained speculative (particularly the AP1 part).

6. IN Figure 6 the authors explored the effect of PTPRK on glycolysis. They concluded that the high glycolytic rate of PTPRK overexpressed cells would support more glucose-derived lipogenesis. While this is certainly plausible, the authors should demonstrate this by isotope tracing from glucose to fatty acids and/or lipids. These can be either radioactive (14C) or stable (13C) isotopes.

7. In Figure 7 the authors compared transcriptional lipogenic signatures in HCC samples with high or low PTPRK. However, in Figure 1 they claimed that PTPRK is high in steatosis and steatohepatitis, but low in HCC. This discrepancy needs to be clarified.

8. Minor point: The authors should adhere to the new nomenclature of fatty liver diseases, not just when discussing MASLD, but also when discussing NASH, now called metabolic dysfunction-associated steatohepatitis (MASH).

Reviewer #3

(Remarks to the Author)
Gilglioni et al report a study that highlights the association of PTPRK with the regulation of metabolism in hepatocytes and provides molecular evidence supporting the relevance of these findings in metabolic liver diseases. The study combines state-of-the-art analytical methods in human samples and mouse and cellular models. Overall, the topic is interesting, the study is well done and provides some relevant results. However, I have a few questions for the authors:

1. There is a very similar study on PTPRG, ref 12 in the manuscript, with overlapping conclusions. The authors need to strengthen the discussion on the role of PTPRK and G and highlight the relevance and novelty of their results in the light of the previous study. Overlapping or specific functions? Both regulate insulin signalling and their reduction improves obesity-related metabolic disorders. While PTPRG has been implicated in inflammatory insulin resistance, does modulation of PTPRK levels have a regulatory role in inflammation that could be associated with the effects observed in this study? Is there cross-talk between the two PTPRs?
2. The size of the groups (humans) is heterogeneous, which could introduce some bias in the analyses; only 2 MASH cases were included, which were mixed with MASH+cirrhosis cases. The distribution of M and F in the experimental groups is heterogeneous, which may be relevant in view of the sex-related differences reported in the studies with the mouse models. Inflammation, diabetes and fibrosis are relevant factors in the progression of chronic liver disease. Information on these factors should be included in the clinical description of patients (Supplementary Table 1).
3. The results shown in Supplementary Figure 1A represent a subset of samples and do not include all samples. For HCC, results are shown for only 2 samples, which is too small for reliable statistical analysis; the results are not commented on in the text. For MASH, out of six cases included, what are the excluded samples, those without cirrhosis?
4. In line 172 it is mentioned that samples within the same stage of the disease showed a similar PTP expression pattern. However, this is not the case for PTPRB, A-2, J and PTPN9.
5. The data supporting the correlations shown in the top panel of Figure 1I are weak.
6. While some of the phenomena described are sex dependent (Figure 3), no major molecular differences are found between male and female mice (Figure 4). The authors should explain this apparent discrepancy. Furthermore, although the average values reported for the levels of the proteins measured by Wb results in statistically significant differences, a remarkable within-group heterogeneity is observed in many analyses that include positive and negative cases.
7. If there is no change in the GSH/GSSG ratio, the increase in GSSG should not be interpreted as an indication of an oxidising environment, but as an increase in overall glutathione levels.
8. It is suggested that targeting and downregulation of PTPRK could be considered for future therapeutic development to treat metabolic liver diseases. However, as this protein is poorly expressed in HCC, the question arises as to whether its silencing would be beneficial in situations that can be considered at risk for liver cancer. Consistent with the reported results, PTPRK expression reported in the Human Protein Atlas (http://proteinatlas.org) is negligible in HCC. However, it is proposed that PTPRK has a favourable prognostic value in kidney cancer and an unfavourable prognostic value in pancreatic cancer, making it difficult to predict what might be the best option for patients with liver disease.
9. In line with the new nomenclature standards, NASH should be renamed MASH (Metabolic disfunction Associated SteatoHepatitis).
10. Lines 527-532. Mass error tolerance must be indicated. It must be specified if the FDR was considered at PSM, peptide and/or protein level.
11. Lines 621-626. Column size, flow rate, mass spec settings and metabolite identification statistics must be indicated.
12. Line 697. The database used must be indicated.

Version 1:

Reviewer comments:

Reviewer #1

(Remarks to the Author)
The authors made a great effort to respond to my concerns and the new version of the paper has plenty of new data. The data provided increases confidence that FBP1 can interact with PTPRK. Although the evidence that FBP1 can be dephosphorylated by PTPRK and more importantly that dephosphorylation of FBP1 mediates the cellular effects of PTPRK are still relatively weak, a role of FBP1 fits all the other data shown. I think this is a very solid paper now, with more than enough data to make an initial strong case.

Reviewer #3

(Remarks to the Author)
The authors answered most of my questions satisfactorily. However, I still have a few recommendations.

I agree with some of the authors' arguments and believe that the potential therapeutic interest of targeting PTPRK would be based on a personalised strategy. To support this hypothesis, additional studies are needed that are beyond the scope of the current investigation and therefore I would recommend to reduce the emphasis in the text.
Proteomics results were filtered with an FDR < 1%. How was the protein inference controlled?

POINT-BY-POINT RESPONSE TO REVIEWERS' COMMENTS

Reviewer #1

This is an interesting, very well written paper focusing on the characterization of the role of PTPRK in hepatocytes. There is a lot of data and the key findings are that PTPRK is upregulated in steatosis and NASH, where it regulates hepatocyte metabolism to promote lipogenesis. This part is elegantly demonstrated via genomics, metabolomics, and in vivo experiments using KO mice and ad-PTPRK expression systems. The authors then provide evidence -unfortunately a bit weak- that such effect of PTPRK is due to dephosphorylation of FBP1, a key glycolysis enzyme. Finally, they report evidence that deletion of PTPRK mildly affects dinitrosamine tumorigenesis in mice. Strengths of the paper are the fact that human specimens and data analysis guided mouse and cell biology experimentation and the meticulous experimentation. However the paper needs a bit more work to support mechanistic conclusions about how PTPRK regulates lipogenesis in hepatocytes.

Major comments

The molecular biology part of the paper (i.e. the identification of a new substrate of PTPRK) is an essential part of the novelty and depth of this paper but is weak at the moment and needs further elaboration and experimentation. Are the site identified exposed in structures of FBP1 (from my preliminary assessment Y265 might have limited exposure)? The models provided need to be shown at much higher resolution and what is the predicted effect of phosphorylation on the structure of FBP1?

We have included higher-resolution images in **Figure 5n** and **Supplementary Figure 7a** showing the exposure of the tyrosine residues to the catalytic site. To clarify this, the substrate specificity of PTPRK is determined by the protein-protein interaction with the pseudophosphatase domain PTPRK-D2 (Hay IM, et al (2022). *eLife* 11:e79855). The function of FBP1 depends on both its expression level and oligomerization state, which fluctuates in an equilibrium between tetramer and dimer. We used FBP1, both the tetramer and the dimer, for the computational analysis of the interaction with PTPRK-D2 (Kozakov D, et al (2017). *Nature Protocols* 12:255-278). The dimer is fully active (Wiśniewski J, et al (2017). *Oncotarget* 8:115420-115433) and we obtained highly populated, low-energy docking patterns that exposed the pY216 and pY265 residues (**Supplementary Figure 7a-f**). For both human and mouse proteins, we obtained up to five models of binding between dimeric FBP1 and PTPRK-D2 (**Supplementary Figure 7a** shows human model 1), whose surface generated a pseudophosphatase domain D2 docking site, allowing access of the D1 catalytic domain to the tyrosine phosphorylated residues. These residues are exposed to the solvent in both subunits of the FBP1 dimer and can therefore serve as substrates for PTPRK-D1 because the linker connecting the D1 and D2 domains is made by a long flexible loop (amino acids 1145-1170 and 1163-1189 in human and mouse, respectively). In the different models, the PTPRK-D2:FBP1 dimer interaction is stabilized by hydrogen bonds, salt bridges, and hydrophobic interactions (**Supplementary Figure 7a**). In the models, the PTPRK-D2:FBP1 dimer complex remains bound (RMSD less than 14 Å) throughout the simulation time (200 ns, Fernández-Ginés R, et al (2022). *Redox Biology* 55:102396), with the exception of the human model 2 (**Supplementary Figure 7b, c**). Solvation binding energy measurements (MM|PBSA, Wang

C, et al (2016). *J Comput Chem* 37:2436-46), shown in **Supplementary Figure 7d, e**, indicate that the binding for the PTPRK-D2:FBP1-PP dimer complexes (pY216, pY265) is stable, especially when considering the last 50 ns of the simulation (MM|PBSA values calculated with YASARA Structure software indicate stronger binding, the more positive the value, Krieger E, et al (2014). *Bioinformatics* 30:2981-2). Residues pY216 and pY265 have no effect on the secondary structure of FBP1 for either the PTPRK-D2-interacting or non-interacting monomer (data not shown). Monitoring the percentages of alpha helix, beta sheet, loops, and coil during the 200 ns molecular dynamics simulation indicated that there were no significant changes in either the phosphorylated or non-phosphorylated protein, nor any differences between the two proteins. In contrast, subtle but repetitive changes in the tertiary structure distinguish phosphorylated from non-phosphorylated FBP1 (**Supplementary Figure 7f**) in all models (except FBP1-PP model 2, which loses its binding to PTPRK-D2). An increased number of H-bonds is detected between the amino acids of the PTPRK-D2:FBP1, pY216, pY265 dimer complex, with no change in the number of H-bonds of the protein complex with the solvent (**Supplementary Figure 7f**). In addition, the radius of the gyration values of the phosphorylated protein are smaller (between 0.5 and 1 Å) than for the non-phosphorylated protein, i.e. phosphorylation increases the compaction and binding stability of the PTPRK-D2:FBP1 dimer complex, and both properties should be lost after the catalytic action of PTPRK-D1. To improve the clarity of the figures, we have modified **Figure 5n** and included additional information in **Supplementary Figure 7a-f**.

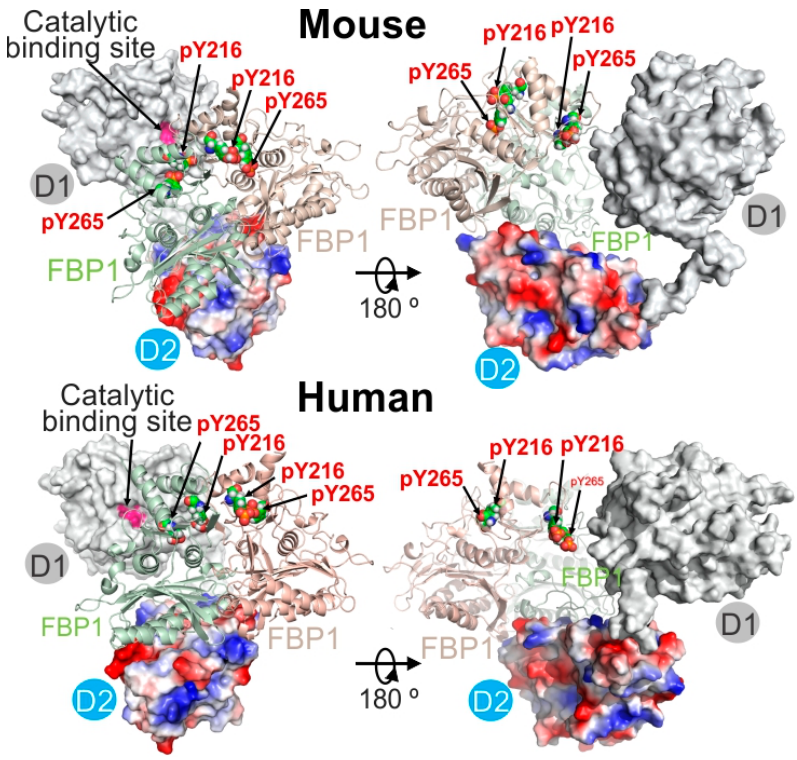

Figure R1 (new Figure 5n in the manuscript): *Conservation mapping of the predicted PTPRK-FBP1 interface, illustrating the PTPRK-D2 complex (red, blue, and grey surface representation of their electrostatic surface potential) interacting with the FBP1 dimer (light green and light red) and the proximity of the PTPRK catalytic site and increased FBP1 phosphotyrosine residues. The D1 domain of PTPRK is shown in grey surface representation.*

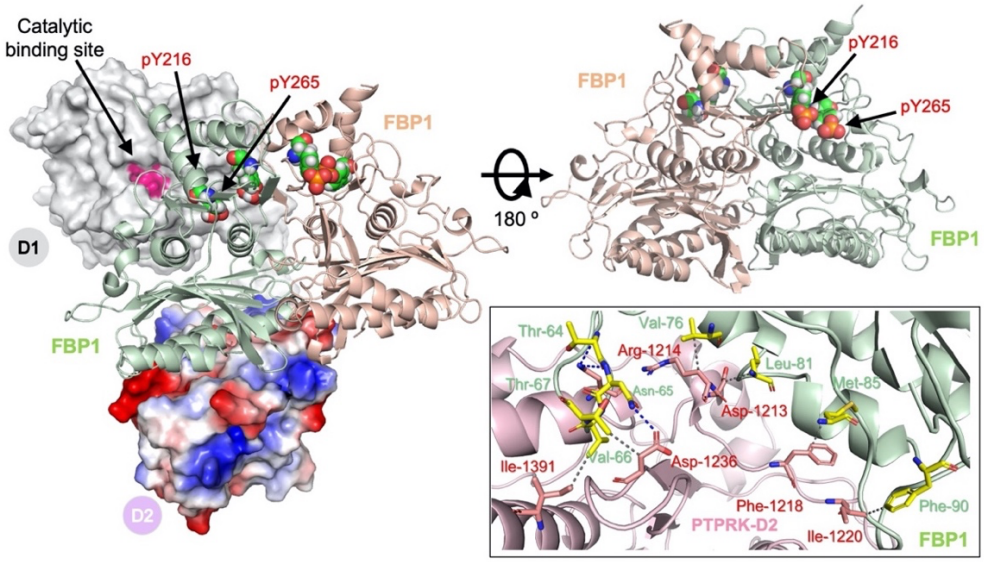

Figure R2 (new Supplementary Figure 7a in the manuscript): *Structural prediction of the PTPRK-D2:FBP1 phosphorylated dimer complex. PTPRK-D2:FBP1 dimer complex phosphorylated after 200 ns of molecular dynamics simulation. The electrostatic potential coloured surface of PTPRK-D2, and the polypeptide backbone of the FBP1-pY216, pY265 dimer are shown. In addition, an open model of PTPRK-D1-D2 (D1 shows the molecular surface in grey) has been superimposed to highlight the proximity of the catalytic site of PTPRK-D1 (lemon) and the pY216, pY265 residues (represented as spheres). Front view of the catalytic site of PTPRK-D1 (removed from the presentation) to show the accessibility of residues FBP1-pY216, pY265 of the cyan-coloured monomer. The PTPRK-D2:FBP1 interface (backbone) is shown and the amino acids (sticks) that stabilize the interaction of the complex are highlighted.*

Much more evidence of FBP1 phosphorylation endogenously as well as dephosphorylation by D1+D2 PTPRK needs to be provided. Ideally also expression of phosphorylation-deficient mutants of FBP1 would be provided in order to support that FBP1 is key in mediating the mechanism of action of PTPRK.

We performed additional experiments to strengthen our evidence supporting FBP1-PTPRK interaction (**page 13**). Thus, the Octet Bio-layer Interferometry (BLI) assays was performed using human His-FBP1 and a His-tagged non-specific protein control immobilized onto Octet-NTA biosensors. Incubation with 200 nM PTPRK resulted in a wavelength shift indicative of binding. Background subtraction confirmed specific binding between PTPRK and FBP1 (**Supplementary Figure 7g**). In addition, HepG2 cells were transfected with plasmids expressing either wild-type or triple tyrosine mutant FBP1-myc (Y265F, Y245F, and Y216F) and treated with pervanadate to enrich phosphotyrosine levels in cell lysates (**Supplementary Figure 7h**). Using purified recombinant His-tagged PTPRK ICD D1057A (Fearnley GW, et al (2019). *eLife* 8:e44597), we conducted pulldown assays and observed stronger binding of wild-type FBP1 compared with the tyrosine mutant (**Supplementary Figure 7i**). Moreover, we performed a co-immunoprecipitation experiment in HepG2 cells overexpressing PTPRK (via adenoviral vector Ad-PTPRK) and transfected with either wild-type or triple tyrosine mutant

FBP1, treated with pervanadate and subjected to immunoprecipitation with anti-Myc magnetic beads. Western blotting analysis of the eluted samples showed stronger Myc pull-down bands in wild-type FBP1 compared to the mutant (**Supplementary Figure 7j**). These results support the interaction between PTPRK and FBP1, which is stronger when FBP1 tyrosine residues are phosphorylated. Furthermore, the western blot analysis using anti-phospho-FBP1 (Y265) antibodies (**Supplementary Figure 8a**), demonstrated phosphorylation of FBP1 at Y265 and the phosphoproteome analysis identified the tyrosines in steatotic freshly isolated mouse hepatocytes (**Figure 5k, l**). Future studies will focus on identifying the tyrosine kinase responsible for this phosphorylation and the associated regulatory signals.

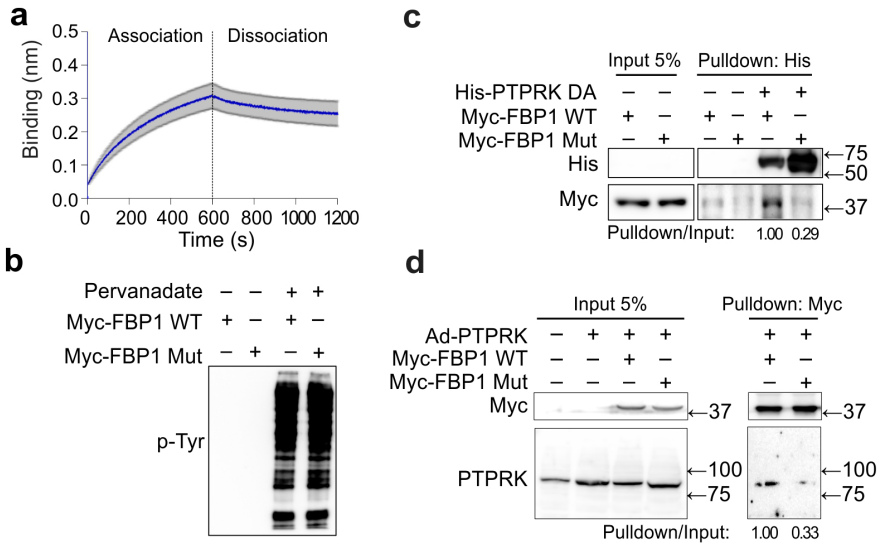

Figure R3 (new Supplementary Figure 7g-j in the manuscript): *(**a**) Human His-FBP1 and a His-tagged nonspecific protein of 22 kDa (negative control) were immobilized onto Octet-NTA biosensors. A wavelength shift (nm) was recorded after incubation with PTPRK at a concentration of 200 nM for 10 min. Subsequently, the protein-bound biosensor was incubated in buffer to measure the dissociation reaction, with background subtraction performed to remove nonspecific binding of PTPRK to the immobilized FBP1. The result is the mean ± SEM of 3 independent experiments. (**b**) HepG2 cells were transfected with plasmids expressing either human FBP1-myc wild-type or a triple tyrosine mutant (Mut, Y265F, Y245F, and Y216F). Western blot showing increased tyrosine phosphorylation in pervanadate-treated samples. (**c**) Recombinant PTPRK pulldown assay. HepG2 cells were transfected with plasmids expressing FBP1-myc wild-type (WT) or triple tyrosine mutant (Mut). Pervanadate-treated HepG2 lysates were incubated with purified recombinant His.TEV.Avi.PTPRK ICD D1057A conjugated to pre-washed Ni-Sepharose His-tagged protein resin at room temperature for 1h on a rotor, followed by immunoblotting with indicated antibodies. The result is representative of 2 independent experiments. (**d**) HepG2 cells were transduced with an adenoviral vector to induce PTPRK overexpression (Ad-PTPRK) and then transfected with plasmids expressing FBP1-myc wild-type (WT) or triple tyrosine mutant (Mut). Pervanadate-treated cells were lysed and immunoprecipitated with anti-Myc magnetic beads, followed by immunoblotting with indicated antibodies. The result is representative of 2 independent experiments.*

Another significant weakness is the lack of any discussion of limitations/inconsistent areas of the study. For example what's the meaning of differences that are only evident when comparing high fat vs low fat hepatocytes within genotypes, or why there is a dissociation

between enzyme and metabolite expression in Fig. 6D, or why the tumorigenesis phenotype in the last figure is so mild (is there any compensation mechanism?)

We have expanded the Discussion to describe limitations of our study (**page 18, 19, 21**). PTPRK-induced metabolic reprogramming in hepatocytes can indirectly affect several other pathways. Fat accumulation in hepatocytes results from perturbations in fat oxidation, synthesis, exportation, dietary intake, and uptake, as well as esterification rates (Bence KK, et al (2021). *Molecular Metabolism* 50:101143). We studied differentially expressed genes by comparing hepatocytes with varying fat contents within each genotype. This approach allowed us to identify modified pathways only present in PTPRK-knockout hepatocytes, such as GAP junction and ECM receptor interaction, which are likely related to the role of PTPRK at the cellular interface. We have included a comment on **page 12**.

Figure 6d (new Figure 8a) reports the metabolite abundance, while information regarding the enzymes in that figure refers to their phosphorylation status analysed in hepatocytes. It is not always known the specific role of phosphorylation in inducing or suppressing enzymatic activity (Humphrey SJ, et al (2015). *Trends Endocrinol Metab* 26:676-687). The dissociation between enzyme levels and substrate abundance can be mediated by phosphorylation and other post-translational modifications that may not correlate directly with enzyme or metabolite levels. Allosteric regulation, subcellular compartmentalization restricting access to substrates, feedback inhibition by product levels, variations in enzyme stability, and degradation rates lead to differences in the steady-state levels of enzymes and substrates. This results in temporal discrepancies in complex, multi-layered regulatory mechanisms controlling enzyme activity and metabolite concentrations in a dynamic cellular environment. We have included a comment on **page 16**.

The relatively mild tumorigenesis phenotype observed in this study can indeed be attributed to several factors, including the detoxification of carcinogens, repair of DNA damage, inhibition of apoptosis in cancer cells, immune response, etc. Based on our current knowledge, PTPRK does not directly impact on all these processes in the liver. Instead, PTPRK facilitates hepatocyte metabolic reprogramming, enhancing cancer cell growth by promoting glycolysis. Thus, while DEN-induced tumours can still initiate and progress in the absence of PTPRK, the decreased glycolytic activity contributes to mitigated tumour growth. This suggests that PTPRK's role in modulating glycolysis influences the aggressiveness of liver tumorigenesis. Although the observed cancer phenotype may appear mild, the initial experiment was conducted in non-obese animals fed with standard chow diet. We have now combined DEN injection with obesogenic HFHFHCD feeding (Broadfield LA, et al (2021). *Cancer Research* 81:1988-2001) and observed a consistent reproducible effect. Specifically, there was a significant reduction in tumour size and area in male (n=18-23) and reduction in tumour number and area in female (n=11-18) mice. This reinforces our finding of the relevance of PTPRK in hepatocyte metabolic reprogramming in obesity. **Figure 7 (now Figure 9)** has been changed to include the results of our tumorigenesis experiments under obesity conditions, **page 17**, and Methods (**page 25**). We have presented the results obtained with male mice under chow or HFHFHCD conditions in the main figure, as HCC is more prominent in males. The results obtained using female mice are presented in **Supplementary Figure 9b-g**. Our experimental outcomes across both sexes and dietary conditions complemented our study of PTPRK in liver tumour development in obesity.

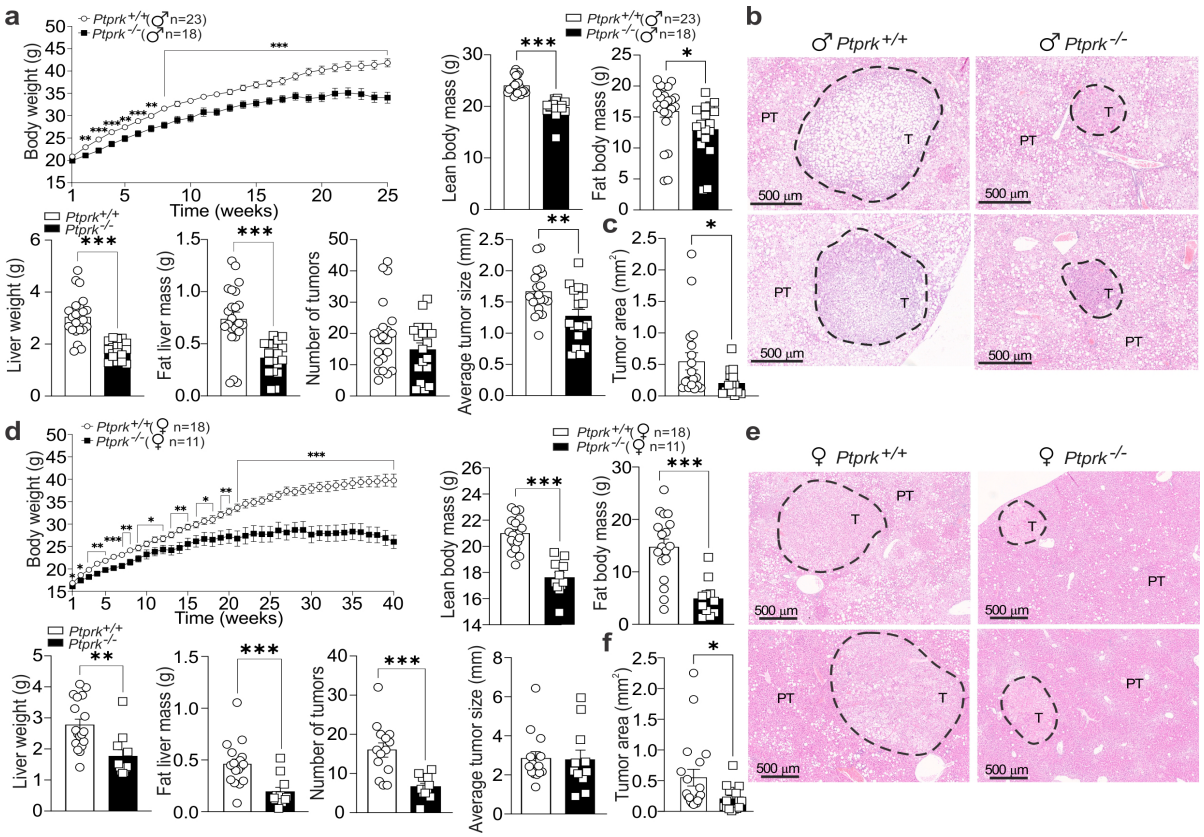

Figure R4 (new Figure 9g-i and Supplementary Figure 9e-g in the manuscript): *Male and female Ptprk$^{-/-}$ and Ptprk$^{+/+}$ mice were subjected to diethylnitrosamine (DEN) induction of liver cancer at 2 weeks of age. At 6 weeks of age, the diet was switched from chow to high-fat high-fructose high-cholesterol diet (HFHFHCD), and tumour development was assessed when the males reached 31 weeks of age (25 weeks on HFHFHCD). For the females, the measurements were performed when they reached 46 weeks of age (40w on HFHFHCD). Body weight was measured weekly throughout the HFHFHCD feeding period (a, d), and body composition, liver weight, and fat liver mass were recorded at the end of the diet treatment (a, d). Tumours on the hepatic lobes were quantified and measured, considering tumours larger than 0.2mm. The results are presented as the number of tumours per liver and average tumour size (a, d). Microscopic tumours were quantified through histological analysis. Representative H&E-stained sections showing the nodules (c, f). Statistical significance (t-test) is indicated as *p<0.05, **p<0.01, ***p<0.001.*

The figures legends needs to be more detailed in explaining 1) the content of the panels, for example Fig. 1F is that protein or mRNA data? 2) What statistics have been utilized in the figure, 3) for non in vivo experiments whether the replicates were done using lines from different mice or same line different experiments or were they technical replicates, 4) where mixed M and F mice have been utilized (Fig. 4E?) and where not.

We have improved the descriptions of the figures. In **Figure 1f**, we state that the data refer to proteins to eliminate any ambiguity (**page 43**). We have included detailed information about the statistical analyses utilized in each figure (**pages 43-50**). For the *in vitro* experiments, we provided clarification regarding the nature of the independent experiment performed. Each

individual value represents independent hepatocyte preparations from different mice. This is now mentioned in the Figure legends (**pages 44, 47-49**) and in Methods (**pages 27, 31**). We have addressed the use of male or female mice in relevant figures, such as **Figure 4e**, and have provided clear indications of the sex of the mice used in each experiment (**pages 45, 46**). There are no results in which males and females were mixed. We appreciate your feedback and believe that these revisions significantly enhance the clarity and comprehensiveness of our figures and figure legends.

Minor comments

1. The figures are too dense and some panels can be eliminated, for example the scheme in Fig. 1C can be replaced by a scheme of PTPRK.

Figure 1c has been replaced with a simplified scheme of the receptor protein tyrosine phosphatases highlighting the ones detected by mass spectrometry analysis.

2. Fig 1 G. The text mentions that the figure only reports PTPRK.

We have corrected the text in the legend of **Figure 1g** (**page 43**).

3. Fig. 1J. IHC is not quantitative and the observation of nuclear-only overexpression is not easily rationalized, also is there any data about the validation of the antibody utilized? This figure ideally needs to be replaced by IF on human or mouse specimens and looking at plasma-membrane vs nuclear pattern.

We previously validated the antibody used for immunohistochemistry by staining wild-type and PTPRK-knockout mouse livers. As expected, staining was observed only in wild-type livers when both primary and secondary antibodies were used, as shown in the top images. Conversely, when only the secondary antibody was used, none of the livers showed positive staining for PTPRK (bottom images). This underscores the specificity of the antibody used in our study.

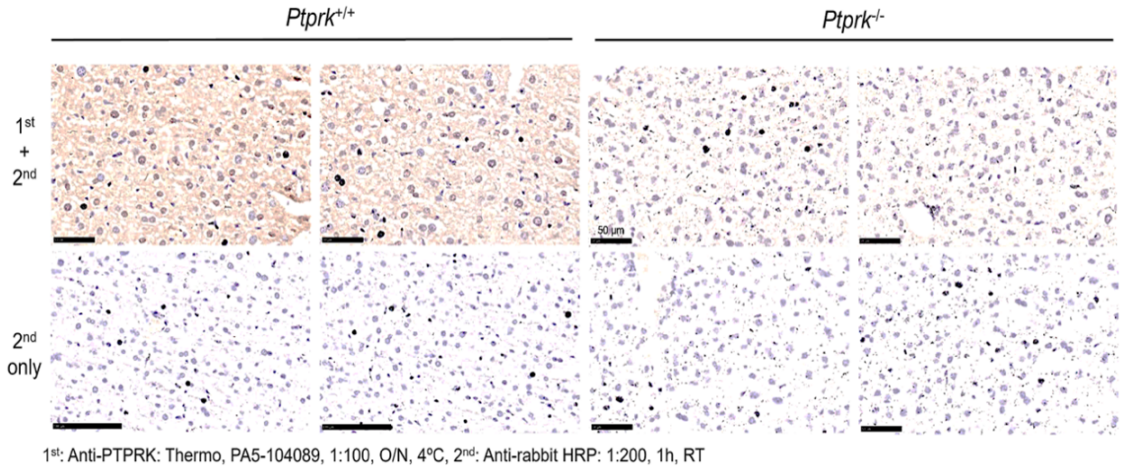

Figure R5: *Representative immunohistochemistry (IHC) images of PTPRK staining in Ptprk$^{+/+}$ and Ptprk$^{-/-}$ mouse livers. The top row displays images obtained using both primary (1st) and*

secondary (2nd) antibodies, while the bottom row shows images obtained using only the secondary antibody to control for the staining method and the specificity of the PTPRK antibody used for IHC. Scale bars 50µm or 100 µm.

PTPRK expression was increased in the cytoplasm and nucleus in human liver disease samples (**Figure 1i**). However, due to the high number of fat vacuoles in steatosis, we did not find a reliable method for quantifying PTPRK cytoplasmic staining; instead, we performed nuclear quantification using Cell Profiler. We have now performed additional experiments using plasmids to overexpress PTPRK in HepG2 cells either the full-length PTPRK protein fused to GFP or only the intracellular domain, to provide a clearer understanding of PTPRK subcellular distribution (**page 7**, **Figure 1j** and Methods (**page 28**). Full-length PTPRK exhibited signals at the plasma membrane, particularly in regions of cell-to-cell contacts and homophilic interactions, as well as in vesicles within the cells. Conversely, the intracellular domain displayed a broad cytoplasmic distribution with a strong signal in the nucleus, which is consistent with previous observations (Anders L, et al (2006). *Molecular and Cellular Biology* 26:3917-34). These findings align with our observations of nuclear PTPRK staining in human slides.

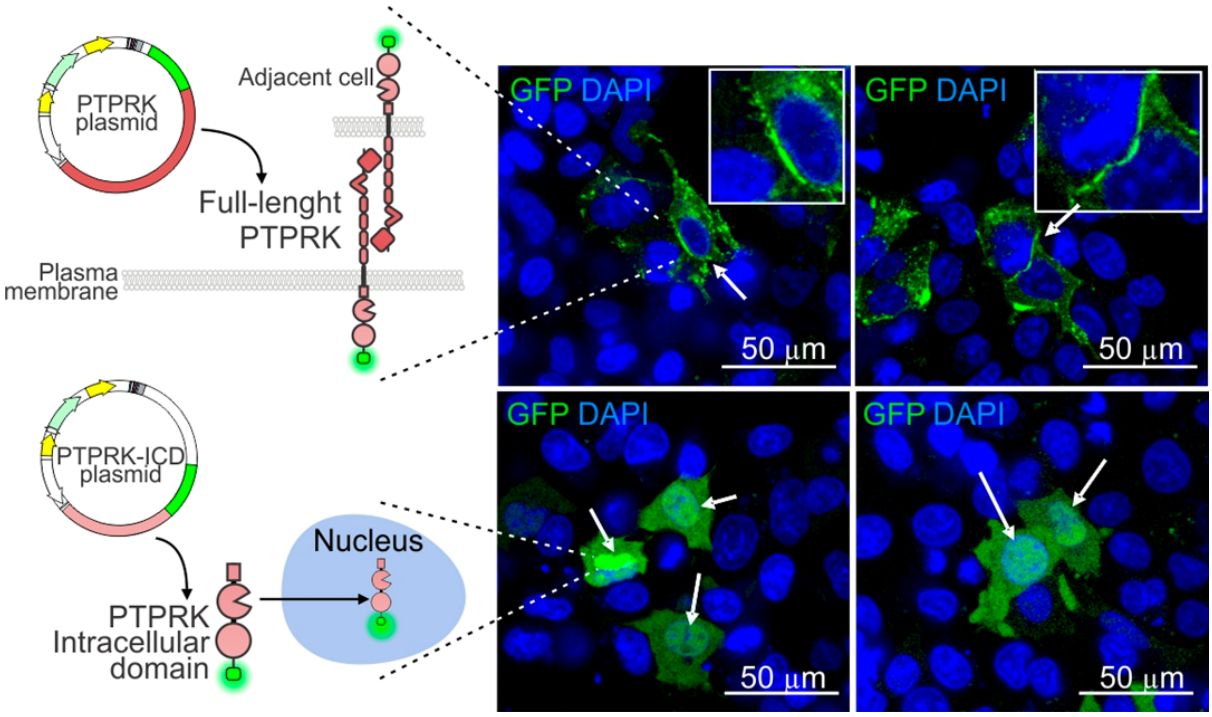

Figure R6 (new Figure 1j in the manuscript): *Cellular localization of recombinant PTPRK. Representative confocal images of HepG2 cells expressing mouse full-length (top row) or the intracellular domain (ICD, bottom row) of PTPRK with a C-terminal mGreenLantern tag (green). The full-length coding sequence of PTPRK or the predicted ICD of PTPRK (exons 16 to 34) fused to mGreenLantern were synthesized by GenScript. The synthesized product was cloned into a pcDNA3.1 plasmid containing the promoter region of the simian cytomegalovirus major immediate early transcription unit IE94 (CMV IE94 promoter). For transfection, HepG2 cells were plated in polymer coverslip bottom plates (Ibidi, #80826) and transfected using Lipofectamine 3000 Transfection Reagent*

(ThermoFisher, L3000008). The day after transfection, cells were fixed and nuclei were stained with DAPI (blue). The images were taken by confocal microscopy (Zeiss LSM780) using one channel for mGreenLantern (GFP) with an excitation wavelength of 488 nm and a second channel for Hoechst with an excitation wavelength of 405 nm. The images were analysed using Zen software (scale bar: 50µm).

4. Fig, 2I. This is a modest increase, how does it compare to the mass spec data in human tissues.

Comparison of western blot and mass spectrometry data with factors such as obesity duration, genetic background, and environmental influences can contribute to differences in PTPRK upregulation in mice and humans. Western blot imaging and mass spectrometry quantification also have different linear ranges, with mass spectrometry having a larger dynamic range for quantification. Despite these inherent differences, we consistently found the same phenotype across the experimental analysis. Our data demonstrate a consistent pattern of change reflecting alterations in PTPRK and the molecular pathways under investigation. Although the magnitude of the increase in PTPRK may vary between mouse models and human samples, the overarching trend remains robust and indicative of the proposed biological processes. While acknowledging the inherent nuances between experimental systems and methods, our findings underscore the relevance of the observed phenotypes and their conservation in the different species.

5. Fig. 2J. The blot seems to show a much higher level of overexpression than even the highest point of the histogram.

Thank you for your feedback. We double-checked the quantification of the blot in **Figure 2j** and confirmed that the protein expression levels are correct.

6. Fig. 4B. There seems to be two groups of animals here for what concerns SREBP1 expression can the authors comment on it.

SREBP1 and ChREBPa expression is intricately linked to nutritional cues, particularly in response to insulin and dietary intake. Given the sensitive nature of SREBP1, ChREBPa (and other metabolic proteins analysed by western blot in **Figure 4**) to nutritional status, we ensured a standardized fasting period of six hours (food was removed at 9 am) in individual cages and clean bedding before liver collection. We carefully controlled the temporal aspects of our experimental setup. Liver samples were collected on the same day (males and females separately) between 3 and 6 pm to minimize circadian influences on gene expression. Additionally, we collected pieces from the same region and lobe (center region of the left lobe) for the analysis, to reduce variability. Despite these efforts, individual variations in animal behaviours, such as pre-fasting food consumption and potential coprophagic behaviour, could contribute to the observed differences. We highlight that the overall changes were significant between the compared groups, and were preserved in both sexes, indicating the mechanism by which PTPRK affects nutrient metabolism in hepatocytes. We have included a comment in **page 11**: “Individual feeding behaviours may influence observed differences in SREBP1, ChREBPα, and other metabolic proteins. However, significant changes were consistent across sexes.”. We have also included the experimental details in Methods, **page 24**: “Mice underwent

a 6h fasting starting at 9 am, with individual housing in cages with clean bedding, and liver samples were consistently taken from the center of the left lobe".

7. Fig. 4 G and H, is any metabolic phenotyping available for these mice?

The aim of this experiment was to assess the effect of hepatic PTPRK overexpression on hepatic fat accumulation and PPARγ expression. We monitored body weight, evaluating body composition at the end of the experiment, performing a glucose tolerance test, and measuring glycemia levels after a 6-h fast period. None of these parameters was significantly affected by the short period of PTPRK expression. We have included a comment on **page 11**.

8. Fig. 5F this figure needs a heading.

We have addressed your suggestion by incorporating a heading in **Figure 5f**, **page 46**. Thank you for bringing this to our attention: "Pellets of the hepatocytes with high-fat content were lysed, proteins precipitated, trypsin-digested, and analysed via LC-MS/MS for total and phosphoproteome."

9. Fig. 7E. The discrepancy between tumor size and area needs some explanation.

The measurement of tumour size in the mouse liver was performed using a calliper, focusing on tumours visible on the liver surface exceeding 0.2 mm in size. This involved averaging 2-3 measurements taken from different angles, depending on the tumour shape. In contrast, tumour area refers to measurements obtained from the histological analysis of liver sections. Following tumour size measurement, sections of the left lobe were collected for histological examination to identify microtumours within the liver that were not visible during macroscopic assessment. These approaches are commonly used to assess liver tumours (Yang T, et al (2016). *Gut* 65:124-33; Lian S, et al (2019). *Gastroenterology* 156:1156-1172; Zhang P, et al (2022). *Cell Metabolism* 34:1359-1376) with each method complementing the other. Differences can be attributed to tumour distribution between the liver surface and its inner regions, as well as to the tumours detected during histological analysis. We have included a comment in the figure legend (**page 50**): "Tumour area measurements were performed using H&E-stained paraffin-embedded liver sections of the left lobe for the identification and measurement of the area of microtumours within the hepatic lobe. Representative H&E-stained sections show the presence of nodules (**e, h**) and tumour area (**f, i**).".

Reviewer #2 (Remarks to the Author):

In this work, Gilglioni et al demonstrated that the tyrosine phosphatase receptor PTPRK is mediating liver lipogenesis, steatosis and potentially HCC mediated by MAFLD.

At first, the authors demonstrated an increase in the expression of several PTPRs, but decided to focus on PTPRK as it is the most abundant PTPR in the liver. It is uniquely induced during hepatic steatosis and steatohepatitis, but then downregulated in HCC. The authors directly linked the expression levels of PPARG with that of PTPRK, and with that, correlated PTPRK with metabolic dysregulations observed in fatty live diseases. Using phosphor-proteomics, they also demonstrated that PTPRK is dephosphorylating the gluconeogenic gene FBP1, and with that fructose-1,6-P2 (the substrate of FBP1) is lower in PTPRK knockout cells, indicative of a negative correlation between PTPRK and FBP1 (inactivation of FBP1 by PTPRK). In line with that, PTPRK overexpression stimulated glycolysis.

While the work provides supporting evidence for their conclusions, it is still somewhat correlative in nature, and lack clarity of the mechanism by which PTPRK is involved with MAFLD.

Specific points to address:

1. A technical point: In the PTP proteomics (Figure 1E & F) the results are presented semi-quantitatively where each PTP is compared to other family members. Using "spectral counts" as the authors did, one cannot compare the abundance of different peptides, as they may be ionized differently and provide different counts. Hence, one can only discuss the relative abundance of each protein under different conditions (comparing the signal of identical peptides). This needs clarifications and a different way to present the data – though the conclusions to continue the focus on PTPRK will not change, as they are eventually based on RNA expression levels.

We thank the reviewer for raising this question. We agree that peptides of different sequences can lead to slight ionization differences, and the more drastically different the peptide sequences, the higher the chance of observing differences in ionization. However, in this context, all PTP catalytic peptides are at least 50% identical in sequence, because PTP catalytic peptides contain the conserved catalytic motif common to all PTPs. Thus, the peptides are at least 50% identical between each other. In addition, the reviewer mentioned that differential ionization leads to different number of spectra counts. We respectfully disagree with this comment; we think ionization mostly affects intensity and is rather unlikely to lead to a complete inability to ionize (zero count). In addition, considering that the peptides are at least 50% identical in sequence, it is even less likely that some peptides will fail to ionize completely. We analysed the data using spectral counting, which is less sensitive to intensity changes than full quantitation, and we think this is the best way to represent this data. We have added a sentence in the Methods (**page 23**): "Spectral counting was utilized to compare relative abundance among different PTPs, considering that peptides containing the conserved catalytic motif are at least 50% identical in sequence, minimizing potential variability in ionization efficiency."

2. The authors did not explain why DMOG was used, and what does it mean to the study. Is PTPRK regulated by dyoxygenases or HIF? The effect of DMOG on PTPRK and PPARG was dramatic nevertheless (more than the Notch inhibitor) and requires explanations.

Dimethyloxalylglycine (DMGO) serves as a HIF stabilizer, given that HIF-driven hepatocyte responses to hypoxia often lead to metabolic changes, such as increased glycolysis and triglyceride accumulation (Gilglioni EH, et al (2018). *Hepatol Commun* 2:299-312), which is consistent with the metabolic phenotype observed following PTPRK deletion. HIF activation in hepatocytes is associated with steatosis and hepatocellular carcinoma (Chen Z, et al (2023). *Signal Transduct Target Ther* 8:70), implying a potential connection to the PTPRK function. Moreover, hypoxia influences cell adhesion components (Koike T, et al (2004). *PNAS* 101:8132-7; Hasan NM, et al (1998). *Br J Cancer* 77:1799-805.), a major function of RPTPs like PTPRK. Our preliminary analysis also revealed HIF-binding motifs in the promoter region of the *PTPRK* gene (data not shown), further supporting our interest in exploring the effects of a hypoxia-mimicking agent on PTPRK and PPARγ expression in hepatocytes. HIF activation by DMOG inhibited PTPRK and PPARγ expression. This unexpected result underscores the notion that although the metabolic phenotypes induced by HIF or PTPRK are similar (such as increased glycolysis and triglyceride accumulation), they are driven by distinct molecular mechanisms. This highlights the critical role of PTPRK in regulating hepatocyte energy metabolism, which operates independently of the molecular mechanisms recruited in response to hypoxia through HIF activation. Thus, the use of DMOG in this study provided valuable insights into the complex interplay between hypoxia, PTPRK, and metabolic regulation in hepatocytes. We included a comment on **page 9** and have expanded the Discussion to clarify this point (**page 18**).

3. In Figure 3 the authors nicely compared the PTPRK knockout to WT mice under obesity conditions. However, the effects, as significant as they may be, are not compared to non-obese mice (chow diet), hence the reader lack the appreciation of the meaning of these effects. This should be presented.

We acknowledge the importance of contextualizing these effects by comparing them to non-obese mice on a chow diet. However, due to space constraints, to simplify and maintain clarity in **Figure 3**, we chose to present the parameters measured exclusively for the obesogenic diet in male and female mice. We have included **Supplementary Figure 3a-d** detailing the same parameters for mice fed the chow diet. This decision was made to prevent overcrowding the already dense **Figure 3** (comment from Reviewer 1) and to maintain readability.

4. While the work initially demonstrates the correlation between PTPRK and PPARG, it was left unclear how much of the observed PTPRK effect on steatosis is actually mediated via PPARG. This is especially important to appreciate the role of FBP1 in the pathophysiology of PTPRK expression in fatty liver. Inhibition or ablation of PPARG in ad-PTPRK expressed hepatocytes (preferably in-vivo) would provide a better understanding.

We thank the reviewer for this suggestion. The experiment was performed in primary mouse hepatocytes with adenovirus-mediated PTPRK overexpression and siRNA-mediated silencing of PPARγ (n=4, independent hepatocyte preparations). Knockdown of PPARγ prevented fat accumulation in the hepatocytes, highlighting its critical role in PTPRK-induced lipogenesis.

Performing the experiment *in vivo* using a combination of adenoviruses was technically impossible, and genetic deletion of PPARγ was also not possible in the timeframe of this rebuttal. Nonetheless, we believe the experiment in primary cells provides significant evidence of the role of PPARγ in the PTPRK phenotype. The results are presented in **Figure 6h, i** (**page 14**) and Methods (**page 33**).

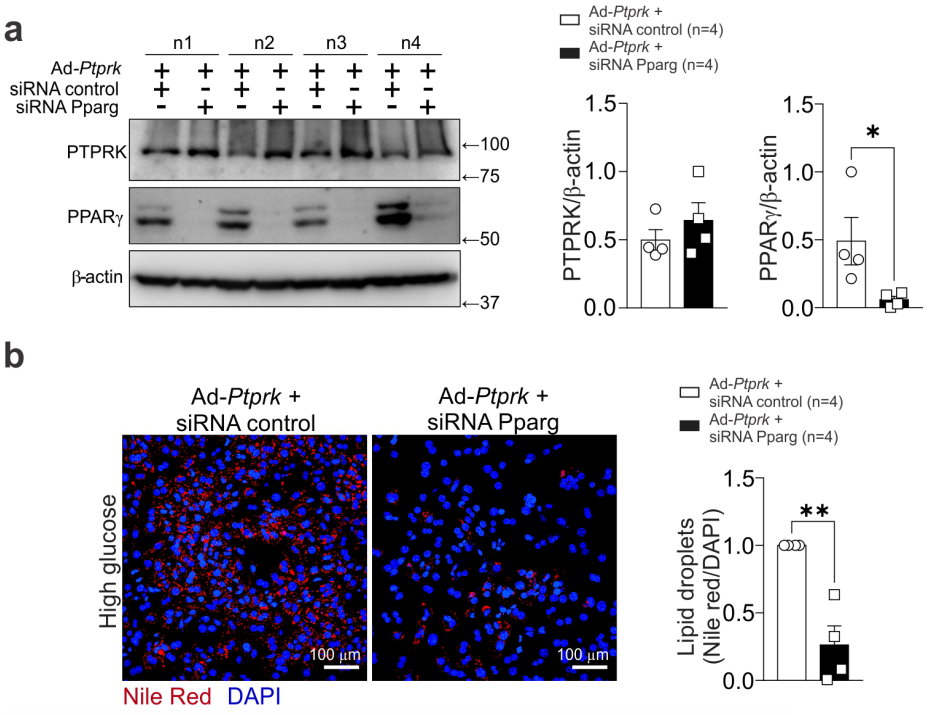

Figure R7 (new Figure 6h, i in the manuscript): *(a) Adenoviral–mediated PTPRK overexpression and PPARγ knockdown in primary mouse hepatocytes were performed followed by exposure to medium containing high concentration (23.5 mM) of glucose. Primary hepatocytes overexpressing PTPRK were transfected with siRNA targeting PPARγ or control siRNA and cultured with high glucose (23.5 mM) for 24h. Immunoblot showing transfection efficiency. (b) Nile red staining was performed to assess lipid droplet accumulation . Statistical analyses were done using two-tailed unpaired Student's t test (a, b) and statistical significance is indicated as *p<0.05, **p<0.01.*

In addition, we hypothesized that elevated glycolysis downstream PTPRK increases PPARγ and channels pyruvate toward acetyl-CoA synthesis, triggering *de novo* lipogenesis. In agreement with our hypothesis, pharmacological FBP1 inhibition enhanced PPARγ and fat accumulation in PTPRK knocked-down primary hepatocytes. Moreover, inhibition of glucose oxidation resulted in decreased PPARγ expression, while PTPRK expression was not affected (**Supplementary Fig. 8b**), supporting our conclusions. The new results are included in **Figure 6j, k** (**page 14**), and Methods (**page 33**).

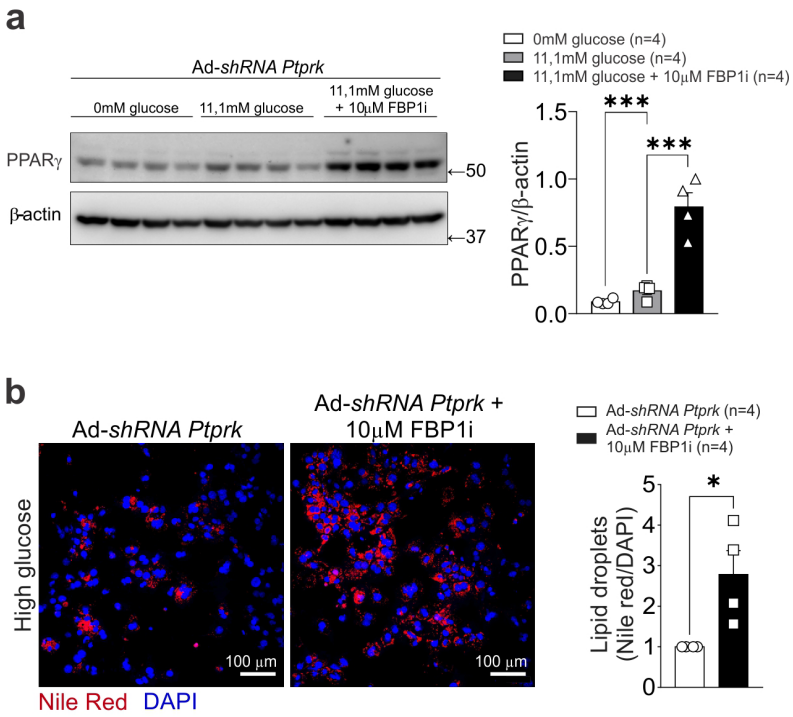

Figure R8 (new Figure 6j, k in the manuscript): *(a) Primary mouse hepatocytes were isolated from C57BL/6 male mice (n=4). After attachment in cell culture plates, the hepatocytes were transduced with an adenoviral vector (Ad-shRNA Ptprk) to knocked down PTPRK. 24h post-infection, cells were treated with medium supplemented with 11.1 mM glucose + 10 μM FBP1 inhibitor, 11.1 mM glucose + DMSO (control), or without glucose for 48h. PPARγ protein levels were measured by immunoblot analysis. (b) Primary hepatocytes were treated with high glucose (23.5 mM) with or without 10 μM FBP1 inhibitor, fixed, and stained with Nile red to visualize lipid droplet abundance. Statistical analyses were done using one-way ANOVA (a) or two-tailed unpaired Student's t test (b) and statistical significance is indicated as *p<0.05, **p<0.01, ***p<0.001.*

5. In Supplementary Figure 5 the authors analyzed AP-1 levels specifically, but later they used RNAseq (Supplementary Figure 6). Nevertheless, it is unclear whether the RNAseq data actually supported their conclusions that PTPRK mediates a transcriptional cascade orchestrated by PPARG and AP1. This remained speculative (particularly the AP1 part).

The rationale for our focus on AP-1 was based on existing literature demonstrating that PPARγ is regulated by this transcription factor (Hasenfuss SC, et al (2014). *Cell Metabolism* 19:84-95). Our RNA-seq data support the notion that PTPRK influences a transcriptional network that includes PPARγ which prompted us to investigate and identify validated PPARγ regulators that are indirectly affected by the sequence of metabolic changes driven by PTPRK. It would be interesting to determine precisely how PTPRK indirectly affects AP-1 protein levels in whole liver lysates, which might also involve changes independent of transcriptional modifications. At this point we speculate that glycolysis stimulation is an important component of this mechanism. Indeed, glycolysis inhibition suppressed PPARγ expression downstream PTPRK (**Supplementary Figure 8b**) and FBP1 inhibition enhanced PPARγ in PTPRK silenced hepatocytes (**Figure 6j**). The study of the detailed mechanism of glycolysis-mediated

PPARγ regulation (and putative AP-1 members), however, is beyond the scope of our manuscript. We have included a comment in the Discussion (**pages 18, 19**), to describe this limitation in our study.

6. In Figure 6 the authors explored the effect of PTPRK on glycolysis. They concluded that the high glycolytic rate of PTPRK overexpressed cells would support more glucose-derived lipogenesis. While this is certainly plausible, the authors should demonstrate this by isotope tracing from glucose to fatty acids and/or lipids. These can be either radioactive (14C) or stable (13C) isotopes.

We used adenoviral vectors to modulate PTPRK expression in primary mouse hepatocytes. These cells were then subjected to high glucose (uniformly labelled with ^{13}C). Immunoblot analyses validated our transduction approach, showing a concurrent increase in PPARγ expression upon PTPRK overexpression. Over a 48h period, we observed a notable reduction in glucose levels in the medium of hepatocytes overexpressing PTPRK, suggesting a heightened glucose oxidation through glycolysis. Nile red staining further sustained our findings, demonstrating a pronounced increase in lipid droplet abundance in PTPRK-overexpressing hepatocytes, confirming our conclusion that elevated PTPRK levels promote lipogenesis and fat deposition in these cells.

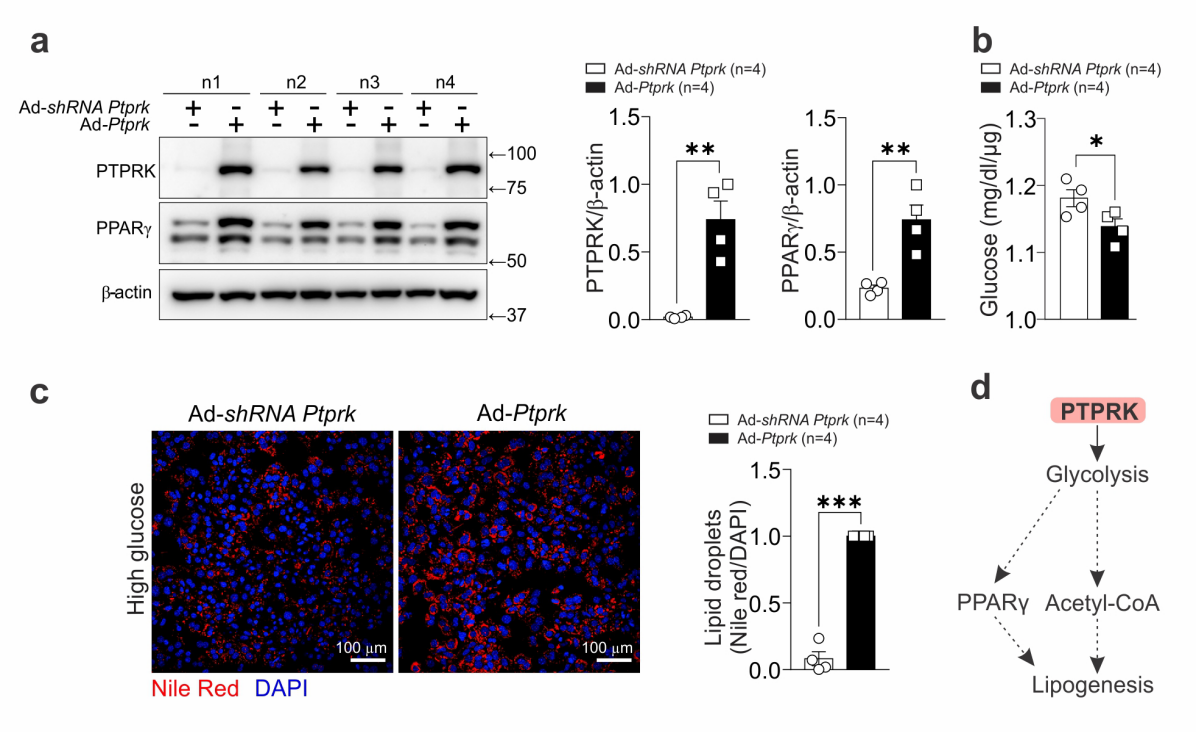

Figure R9 (new Figure 6d-g in the manuscript): *Adenoviral–mediated PTPRK overexpression or knockdown in primary mouse hepatocytes was performed followed by exposure to medium with high concentration (23.5 mM) of ^{13}C labelled glucose. (a) Immunoblot analysis showing PTPRK and PPARγ protein levels. (b) Glucose levels in the medium measured after 48h. (c) The cells were fixed and stained with Nile red to show lipid droplet abundance (d) Schematic representation of the postulated PTPRK mechanism in*

*hepatocytes, illustrating its role in modulating glycolytic activity, PPARγ and lipid metabolism. Statistical analyses were done using two-tailed unpaired Student's t test (a, b, c) and statistical significance is indicated as *p<0.05, **p<0.01, ***p<0.001.*

In our metabolite tracing experiments comparing the effects of PTPRK overexpression and silencing (samples described above) on glycolytic flux in hepatocytes, we analysed key glycolytic intermediates to elucidate the glucose contribution to the formation of these intermediates and related metabolites. Our results showed that hexose bisphosphate, primarily represented by fructose 1,6-bisphosphate exhibited increased abundance and fractional contribution under PTPRK overexpression. The increased fractional contribution of labelled carbon in fructose 1,6-bisphosphate under PTPRK overexpression conditions points to higher glucose uptake and utilization, as well as increased incorporation of labelled glucose into the glycolytic pathway, which is consistent with reduced FBP1 activity. Furthermore, dihydroxyacetone phosphate and glyceraldehyde 3-phosphate, both downstream products of fructose 1,6-bisphosphate, showed increased levels under PTPRK overexpression, as well as phosphoenolpyruvate, indicating enhanced conversion of glyceraldehyde 3-phosphate through the latter stages of glycolysis. This is consistent with the overall action of glycolytic enzymes and a more active glycolytic flux, indicating a metabolic reprogramming toward enhanced glycolysis in PTPRK-overexpressing hepatocytes. Despite intermediated of the TCA cycle trending toward higher abundance in PTPRK-overexpressing hepatocytes, no significant differences were observed in either abundance or fractional contribution. This agrees with our conclusion that the increased flow of carbons from elevated glycolytic rates likely reaches steady state, with excess carbons being directed toward triglyceride synthesis following fatty acid synthesis. Analysing acetyl-CoA and free CoA levels revealed an increased fractional contribution with PTPRK overexpression, although their abundances remained unchanged. The significant enrichment of both acetyl-CoA and free CoA indicates that CoA biosynthesis was also stimulated, and the glucose-derived carbons were eventually converted into ribose-5-phosphate and then ATP, which is used to synthesize CoA, suggesting a higher demand for CoA likely due to its essential role in fatty acid metabolism. We believe that these results have significantly strengthened our observations and demonstrate with the use of ^{13}C tracer the increased glucose use to sustain a high glycolytic rate leading to enhanced lipid production in the cells. We have included the new data as **Figure 6d-f** and **Figure 7** (**pages 14 and 15**), Methods (**pages 31, 32**), and expanded the Discussion (**pages 18-20**).

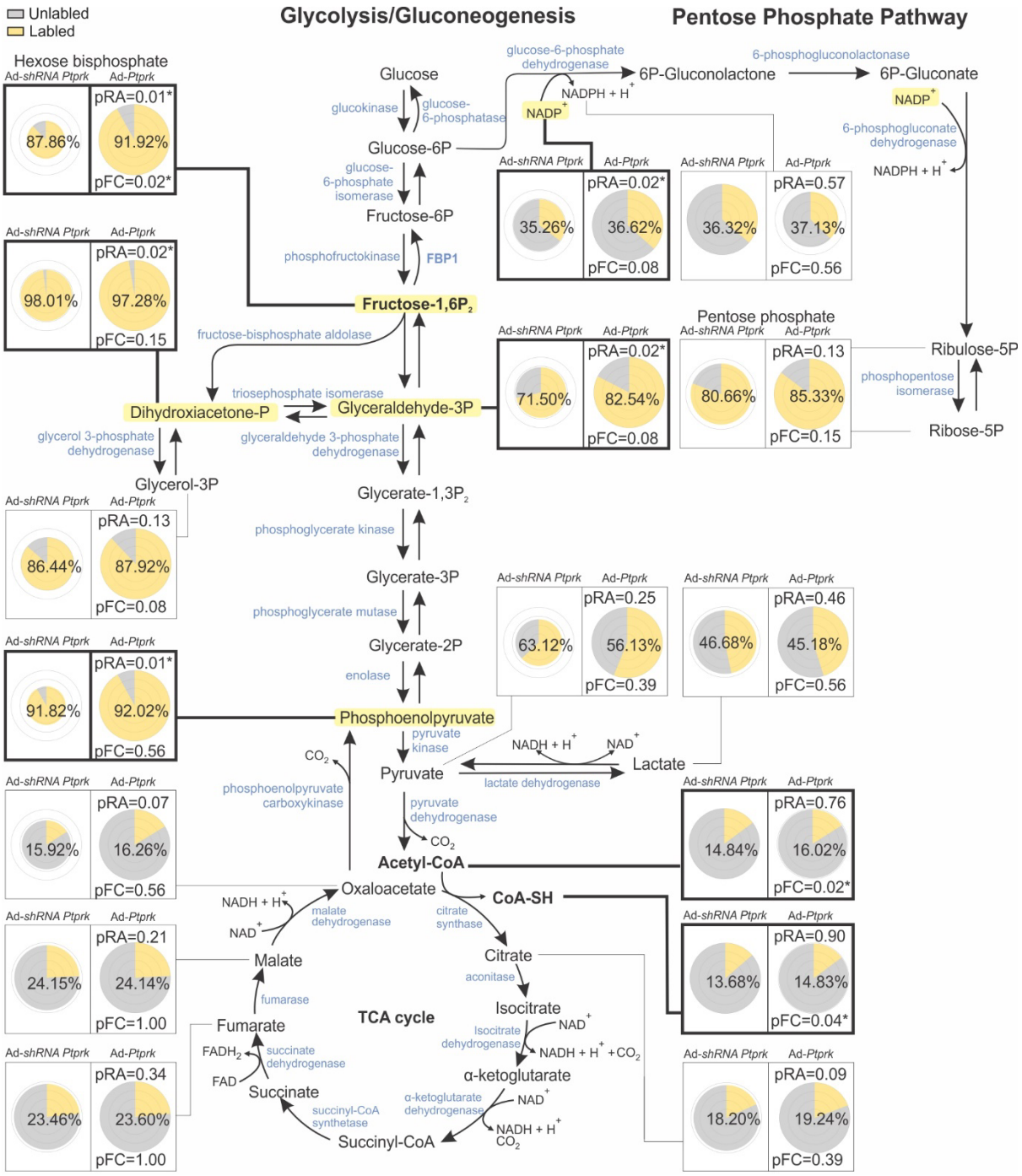

Figure R10 (new Figure 7 in the manuscript): *Pie chart visualizations by Travis Pies applied to 2 cohorts: Ad-shRNA Ptprk and Ad-Ptprk. For each metabolite, the pie radii correspond to the relative abundance, which can be compared between the cohorts of this metabolite. The concentric circles correspond from center outwards to 0.25, 0.5, 0.75, and 1 time the largest abundance. Both the labelled surface fraction of the pie and the percentage displayed in the middle of each pie reflect the fractional contribution. pRA and pFC indicate significance of the difference in respectively the relative abundance (t-test) or fractional contribution (Kruskal-Wallis) with Ad-shRNA Ptprk (* indicates a p value <0.05).*

7. In Figure 7 the authors compared transcriptional lipogenic signatures in HCC samples with high or low PTPRK. However, in Figure 1 they claimed that PTPRK is high in steatosis and steatohepatitis, but low in HCC. This discrepancy needs to be clarified.

We appreciate the opportunity to clarify our findings. Our proteomic analysis of human samples revealed increased PTPRK levels in conditions such as steatosis and steatohepatitis. Similar trends were observed in mouse models of liver dysfunction induced by obesogenic diets, as shown in **Figure 2**, allowing us to characterize this phenomenon. As we expanded our study by analysing large publicly available datasets, we observed a wider spectrum of PTPRK particularly evident in HCC patients. Although PTPRK expression was elevated in several samples, we also identified patients with low PTPRK expression. This diversity in PTPRK levels across larger cohorts underscores the heterogeneous nature of the disease, where different molecular signatures and pathways may be active in distinct patient subgroups, as demonstrated by the positive correlations of high PTPRK with glycolytic and lipogenic signatures. Our experiments in **Figure 2l-p** illustrate how PTPRK expression in hepatocytes can be modulated by various signals, such as time in culture, Notch inhibition, LSP, and DMOG. Furthermore, it is plausible to speculate that other signals as cytokines, hepatokines, and hormones that dynamically change throughout the progression from MASLD to MASH, cirrhosis, and HCC may also influence PTPRK expression and contribute to the observed differences in PTPRK levels. Therefore, the apparent discrepancy can be attributed to the heterogeneous nature of metabolic liver disease and the diversity of pathways in MASLD that can result in the development of HCC, albeit via different mechanisms. We have expanded the Discussion, **page 21**.

8. Minor point: The authors should adhere to the new nomenclature of fatty liver diseases, not just when discussing MASLD, but also when discussing NASH, now called metabolic dysfunction-associated steatohepatitis (MASH).

The entire manuscript, including both figures and text, has been adjusted to align with the most recent nomenclature standards (Rinella ME, et al (2023). *Hepatology* 78:1966-1986). Specifically, in addition to adhering to the new nomenclature for metabolic dysfunction-associated fatty liver disease (MASLD), we have also incorporated the updated term for non-alcoholic steatohepatitis (NASH), which is now referred to as metabolic dysfunction-associated steatohepatitis (MASH).

Reviewer #3 (Remarks to the Author):

Gilglioni et al report a study that highlights the association of PTPRK with the regulation of metabolism in hepatocytes and provides molecular evidence supporting the relevance of these findings in metabolic liver diseases. The study combines state-of-the-art analytical methods in human samples and mouse and cellular models. Overall, the topic is interesting, the study is well done and provides some relevant results. However, I have a few questions for the authors:

1. There is a very similar study on PTPRG, ref 12 in the manuscript, with overlapping conclusions. The authors need to strengthen the discussion on the role of PTPRK and G and highlight the relevance and novelty of their results in the light of the previous study. Overlapping or specific functions? Both regulate insulin signalling and their reduction improves obesity-related metabolic disorders. While PTPRG has been implicated in inflammatory insulin resistance, does modulation of PTPRK levels have a regulatory role in inflammation that could be associated with the effects observed in this study? Is there cross-talk between the two PTPRs?

Thank you for your comment regarding the relevance of our study compared with previous research on PTPRG (Brenachot X, et al (2017). *Nature Commun* 8:1820). PTPRK is a member of the R2B family of PTPs and mediates cell adhesion and signalling via its extracellular and intracellular phosphatase domains, featuring a meprin-A5 antigen-PTP mu (MAM) domain, Ig-like domain, and four FN3 repeats. These structural components, along with a transmembrane domain and cadherin-like sequence, facilitate distinct shapes favouring homophilic interactions for cell-cell contact (Hay IM, et al (2023). *J Biol Chem* 299:102750). In contrast, PTPRG, which belongs to the R5 group of RPTPs, possesses an extracellular domain consisting of a carbonic anhydrase-like (CAH) domain, a single FN3-like domain, and a long, disordered spacer region. The CAH domain lacks the critical histidine residues essential for catalytic activity, suggesting a non-catalytic role, potentially as an HCO_3^- sensor in cellular processes. Additionally, the distinctive intracellular domain organization of RPTPs, including PTPRG, allows for the regulation of catalytic activity through dimerization, with PTPRG potentially forming an inactive dimer characterized by electrostatic interactions and domain occlusion that hinder substrate access (Boni C, et al (2022). *Biomolecules* 12: 84). Although both PTPRG and PTPRK are involved in metabolic disorders, our study elucidates a different mechanism. PTPRG's role in inflammation and insulin resistance was showed by its upregulation in obese/T2DM settings, while PTPRK's involvement in dysregulated hepatic lipid metabolism and glycolysis offers new insights into obesity-associated liver diseases. In contrast to PTPRG established link with inflammation-induced insulin resistance, our study demonstrated the role of PTPRK in metabolic reprogramming and tumorigenesis. The PTPRG role in inflammation was well-documented Brenachot X, et al (2017). *Nature Commun* 8:1820. We measured markers of inflammation, including TNFα, CD68, and F4/80, in the livers of *Ptprk*$^{-/-}$ and *Ptprk*$^{+/+}$ mice after high-fat high-fructose high-cholesterol diet, and no differences were found (results showed below). This suggests that the metabolic effects of PTPRK may be independent of the direct modulation of these inflammatory markers. However, a more detailed analysis of inflammation would be required, which is beyond the scope of the present study.

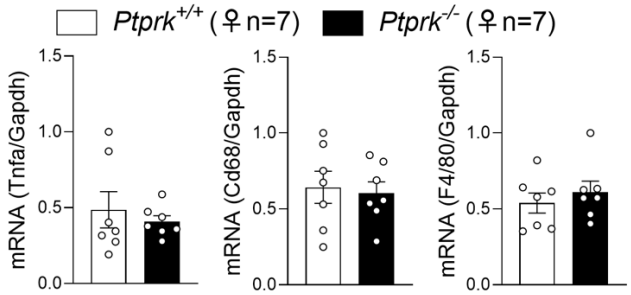

Figure R11: *Liver mRNA expression of inflammation markers. Female (♀) Ptprk*$^{-/-}$ and *Ptprk*$^{+/+}$ *mice aged 8 weeks, were fed a high-fat, high-fructose, high-cholesterol diet (HFHFHCD) for 12 weeks. Following the diet, liver samples were harvested and RNA was extracted. Real-time PCR analysis was conducted to determine the hepatic mRNA expression levels of tumour necrosis factor-alpha (Tnfa), cluster of differentiation 68 (Cd68), and F4/80.*

In conclusion, both PTPRG and PTPRK represent potential therapeutic targets for mitigating insulin resistance and associated complications in obesity-related disorders, albeit likely through distinct mechanisms and substrates. Investigating the therapeutic potential of targeting both phosphatases concurrently, possibly along with other interventions, may provide avenues for addressing obesity-related metabolic disorders and their associated complications. While speculating potential mechanisms that integrate their functions is plausible, our study is complementary, and significantly advances our understanding of receptor phosphatases and the development of hepatic metabolic disorders. We included a comment in the Discussion, **page 21**.

2. The size of the groups (humans) is heterogeneous, which could introduce some bias in the analyses; only 2 MASH cases were included, which were mixed with MASH+cirrhosis cases. The distribution of M and F in the experimental groups is heterogeneous, which may be relevant in view of the sex-related differences reported in the studies with the mouse models. Inflammation, diabetes and fibrosis are relevant factors in the progression of chronic liver disease. Information on these factors should be included in the clinical description of patients (Supplementary Table 1).

We agree that a larger cohort would allow for sample stratification according to gender, BMI, and disease. We plan a future follow-up study with a larger sample size to avoid the gender heterogeneity among the groups. In the present study, in most relevant experiments conducted in mice, we have used both males and females. Importantly, human liver samples, albeit limited, supported our discoveries in mouse and *in vitro* models. We have included the steatosis and fibrosis scores. The steatosis score (as measured according to the criteria from the NAS (NAFLD Activity Score) system, assigning points for steatosis with 0 points for less than 5% of hepatocytes affected by steatosis, 1 point for 5% to 33% affected, 2 points for 34% to 66% affected, and 3 points for more than 66% affected. The fibrosis score system categorizes fibrosis from F0 to F4. F0 indicates no fibrosis, while F1 denotes periportal or perisinusoidal fibrosis. F2 represents both periportal and perisinusoidal fibrosis with occasional bridging, while F3 indicates bridging fibrosis. F4 indicates the presence of cirrhosis. The inclusion of this information provides a more comprehensive clinical description of patients, thereby

allowing for a better understanding of disease characteristics. Besides the complementation of Supplementary Table 1, we mentioned the limitations of the present work and the need for future study with a larger number of human samples in the Discussion (**page 21**).

ID	Biopsy health status	Age	Weight (kg)	Height (cm)	BMI (kg/m^2)	Type 2 diabetes	Gender	Steatosis	Fibrosis	Experiment
CHR01	Healthy liver	80	46	175	15	No	M	0	F0	MS/IHC
CHR02	Healthy liver	66	62	150	28	No	F	0	F0	MS/IHC
CHR03	Healthy liver	28	66	170	23	No	F	0	F0	IHC
CHR04	Healthy liver	63	66	165	24	No	F	0	F0	MS/IHC
CHR08	Steatosis	53	86	185	25	Yes	F	2	F0	MS/IHC
CHR09	Steatosis	39	80	158	32	No	F	1	F0	MS/IHC
CHR10	Steatosis	56	67	173	22	No	M	1	F0	MS/IHC
CHR11	Steatosis	36	82	160	32	No	F	1	F0	MS/IHC
CHR12	Steatosis	61	76	159	30	No	F	2	F0	IHC
CHR13	Steatosis	68	115	168	41	Yes	M	1	F0	IHC
CHR14	MASH/cirrhosis	61	113	179	35	Yes	M	1	F4	MS/IHC
CHR16	MASH/cirrhosis	46	79	156	32	No	F	2	F4	MS/IHC
CHR17	MASH/cirrhosis	48	76	160	30	No	M	2	F4	MS/IHC
CHR18	MASH/cirrhosis	60	80	149	36	Yes	F	1	F4	MS/IHC
CHR19	MASH	46	80	157	32	Yes	F	3	F1	MS
CHR20	MASH	45	85	156	35	Yes	F	2	F1	MS
CHR05	HCC	83	79	175	26	No	M	1	F4	MS
CHR06	HCC	76	76	165	28	No	M	1	F0	MS
CHR07	HCC	43	43	170	19	No	M	0	F4	MS

Table R1 (new Supplementary Table 1 in the manuscript): *Clinical and demographic characteristics of patients from whom liver biopsies were collected and used for mass spectrometry (MS) or PTPRK immunohistochemistry (IHC) analysis shown in Figure 1.*

3. The results shown in Supplementary Figure 1A represent a subset of samples and do not include all samples. For HCC, results are shown for only 2 samples, which is too small for reliable statistical analysis; the results are not commented on in the text. For MASH, out of six cases included, what are the excluded samples, those without cirrhosis?

We thank the reviewer for raising this question. We did not exclude samples of a specific subtype. The exclusion criteria were samples that did not pass all quality controls for reliable total proteome analysis. We included the heat map profile of the HCC samples (**Supplementary Figure 1a and 9a**) but would like to clarify that no pathway or statistical analysis was performed using these two samples. Two HCC samples are indeed few, but this was all the samples that we had, that were of high quality for the global proteome. We felt that although two samples in a category is few, it was more critical to have good quality for high confidence over quantity. A comment was included when presenting these data in Results, **page 6**: "All samples except 1 HCC and 2 MASH passed total proteome quality control for heatmap analysis. HCC samples were not considered for pathway analysis due to low sample size.".

4. In line 172 it is mentioned that samples within the same stage of the disease showed a similar PTP expression pattern. However, this is not the case for PTPRB, A-2, J and PTPN9.

We have modified the text (**page 7**) to better describe the PTP changes, as correctly suggested by the reviewer.

5. The data supporting the correlations shown in the top panel of Figure 1I are weak.

We have followed the suggestion of the reviewer and removed the panel. The correlation between PTPRK and PPARG is now shown in **Supplementary Figure 2a**. The text was updated accordingly (**page 8**).

6. While some of the phenomena described are sex dependent (Figure 3), no major molecular differences are found between male and female mice (Figure 4). The authors should explain this apparent discrepancy.

The sex-specific difference observed in **Figure 3** was a reduction in body lean mass in knockout females, which was not observed in males. This reduction in body lean mass in females is likely due to the higher energy expenditure of PTPRK-knockout mice, which manifests in females as reduced body weight due to lower body fat and lean mass. Sex differences in hormones and their role in body lean mass is likely to contribute to these differences but do not necessarily imply distinct molecular mechanisms for PTPRK action based on sex, as shown in **Figure 4**. While these minor sex differences are noted, the major disparities observed are between genotypes due to the presence or absence of PTPRK. Indeed, extending the feeding leads to similar changes in males and females, with dramatic differences in body weight gain, as revealed by new experiments included in the revised version of our manuscript (**Figure 9**), **page 17**.

Furthermore, although the average values reported for the levels of the proteins measured by Wb results in statistically significant differences, a remarkable within-group heterogeneity is observed in many analyses that include positive and negative cases.

Given the sensitivity of these proteins to nutritional status, we ensured a standardized fasting period of six hours in individual cages with clean bedding before liver collection. Despite these controls, variations in individual animal behaviour, such as pre-fasting food consumption and potential coprophagic behaviour, could influence these differences. Our experimental setup was conducted within the light cycle between 15:00 and 17:00 to minimize circadian effects on gene expression. Additionally, we consistently collected samples from the same lobe (left) to reduce variability. However, individual nuances in feeding behaviour can still introduce variability. We have included a comment in Results, **page 11**.

7. If there is no change in the GSH/GSSG ratio, the increase in GSSG should not be interpreted as an indication of an oxidising environment, but as an increase in overall glutathione levels.

We agree with the reviewer that the stability of the GSH/GSSG ratio in the presence of increased GSSG levels does not necessarily signify an oxidizing environment, and it could

instead indicate an increase in overall glutathione levels within the cell. We have changed the sentence (**page 16**) corresponding to the interpretation that extrapolates the finding of higher GSSG levels as a sign of a more oxidized environment in *Ptprk*$^{-/-}$ livers.

8. It is suggested that targeting and downregulation of PTPRK could be considered for future therapeutic development to treat metabolic liver diseases. However, as this protein is poorly expressed in HCC, the question arises as to whether its silencing would be beneficial in situations that can be considered at risk for liver cancer. Consistent with the reported results, PTPRK expression reported in the Human Protein Atlas (http://proteinatlas.org) is negligible in HCC. However, it is proposed that PTPRK has a favourable prognostic value in kidney cancer and an unfavourable prognostic value in pancreatic cancer, making it difficult to predict what might be the best option for patients with liver disease.

Our findings suggest that PTPRK could potentially serve as a preventive strategy against HCC by reversing or reducing MAFLD and its progression to HCC. We observed (**Figure 9a**) that a subset of patients with high hepatic PTPRK expression may benefit from PTPRK-directed therapy. However, we also identified HCC patients with low PTPRK expression (**Figures 1d, 9a**). Thus, a personalized approach aligns with the concept of individualized medicine, recognizing the heterogeneity of diseases like MASLD-induced HCC and emphasizing tailored treatment strategies for optimal outcomes. Moreover, by delving into the molecular mechanisms underlying PTPRK's metabolic effects, we expanded our understanding of the complex liver diseases in obesity. Nonetheless, we agree that although targeting PTPRK may hold therapeutic potential for metabolic liver diseases, careful consideration must be given to the potential implications for cancer risk in other organs. We have expanded the Discussion, **page 21**.

9. In line with the new nomenclature standards, NASH should be renamed MASH (Metabolic disfunction Associated SteatoHepatitis).

The entire manuscript, including both figures and text, has been adjusted to align with the most recent nomenclature standards (Rinella ME, et al (2023). *Hepatology* 78:1966-1986). Specifically, in addition to adhering to the new nomenclature for metabolic dysfunction-associated fatty liver disease (MASLD), we have also incorporated the updated term for non-alcoholic steatohepatitis (NASH), which is now referred to as metabolic dysfunction-associated steatohepatitis (MASH).

10. Lines 527-532. Mass error tolerance must be indicated. It must be specified if the FDR was considered at PSM, peptide and/or protein level.

We thank the reviewer for pointing this out. We used 1% peptide FDR. This has been amended in Methods (**page 23**).

11. Lines 621-626. Column size, flow rate, mass spec settings and metabolite identification statistics must be indicated.

We have updated the section "LC-MS Metabolomics Analysis" in Methods section to include the column size, flow rate, mass spec settings, and metabolite identification statistics as requested (**pages 31 and 32**).

12. Line 697. The database used must be indicated.

Thank you for your observation. We have included the following sentence in Methods (**page 30**): “For all datasets, the search was performed against the UniProt mouse database (UP000000589).”

POINT-BY-POINT RESPONSE TO REVIEWERS' COMMENTS

Reviewer #1 (Remarks to the Author)

The authors made a great effort to respond to my concerns and the new version of the paper has plenty of new data. The data provided increases confidence that FBP1 can interact with PTPRK. Although the evidence that FBP1 can be dephosphorylated by PTPRK and more importantly that dephosphorylation of FBP1 mediates the cellular effects of PTPRK are still relatively weak, a role of FBP1 fits all the other data shown. I think this is a very solid paper now, with more than enough data to make an initial strong case.

We thank the reviewer for their positive assessment of our manuscript. We agree that additional studies are required to understand the role of PTPRK-dependent dephosphorylation at the tyrosine residues of FBP1 and how this affects enzymatic activity. Moreover, we cannot rule out the direct or indirect regulation of additional enzymes in the glycolytic pathway by PTPRK. We have removed Supplementary Figure 8a, and included a comment in the Discussion (pages 19 and 20) to clarify the limitations of our study: "Further research is needed to explore the precise implications of tyrosine phosphorylation on FBP1. It is crucial to identify the tyrosine kinases responsible for FBP1 phosphorylation and to examine the potential role of substrate cycling in glycolysis in maintaining energy homeostasis. Additionally, we cannot rule out direct or indirect regulation of additional enzymes by PTPRK in the glycolytic pathway that contribute to the phenotype."

Reviewer #3 (Remarks to the Author)

The authors answered most of my questions satisfactorily. However, I still have a few recommendations.

I agree with some of the authors' arguments and believe that the potential therapeutic interest of targeting PTPRK would be based on a personalised strategy. To support this hypothesis, additional studies are needed that are beyond the scope of the current investigation and therefore I would recommend to reduce the emphasis in the text.

We agree with the reviewer and have toned down the therapeutic potential of our findings in the Abstract (page 2) and Discussion (pages 21).

Proteomics results were filtered with an FDR < 1%. How was the protein inference controlled?

We controlled protein inference using MaxQuant's built-in algorithms. MaxQuant uses the target-decoy strategy to generate a decoy database by reversing the peptide/protein sequences in the target database. For protein inference, high-confident peptides were mapped to protein groups, with 1% FDR applied at both the peptide and protein levels to reduce the false-positive identifications. This provides stringent identification while addressing the challenges associated with shared peptides and protein homology.

Although false protein hits are still possible when a single peptide is ued for identification, we also filtered our data using at least 2 unique peptides as filtering criteria for protein identification and found no impact on our conclusions.